

ODD AND EVEN SYMMETRY OF ATMOSPHERIC CIRCULATION—THEORETICAL BASIS AND CLIMATIC CHARACTERISTICS*

Guan Zhaoyong (管兆勇), Xu Jianjun (徐建军) and Wang Panxing (王盘兴)

Nanjing Institute of Meteorology, Nanjing 210044

Received June 11, 1992; revised December 20, 1993

ABSTRACT

Analysis is done of the distribution of odd and even symmetric components of circulations on a global basis in terms of observations and technique for the odd / even symmetry, indicating that climatic features of the component patterns and their temporal evolution are able to reveal their influence of land-sea discrepancy in the Northern and Southern Hemispheres, the time scale of atmospheric response to radiation heating, circulation waveform structure and seasonal adjustment of global circulation.

Key words: atmospheric circulation, symmetry, theoretical basis, climatic characteristics

1. INTRODUCTION

If we view the state of global mean circulations on a meteorological basis, the most striking features for both hemispheres (Palman, and Newton 1969; Pogoxin 1972) are their symmetry and asymmetry about the equatorial plane, which are also called even and odd symmetry, respectively, but will be hereafter referred customarily to as odd and even symmetry (OES). These features are clearly shown in the mean circulations at different levels and marked by noticeable seasonal change, the latter being actually indicative of OES manifestation on a temporal basis.

Dynamically, atmospheric circulation OES has its origin in the OES of the major controlling factors (Yeh and Zhu 1958). The earth's rotation denoted by the Coriolis parameter $f=2\Omega\sin\phi$ may be viewed as a kind of odd symmetric effects; the earth's revolution and the inclination of its axis with respect to the ecliptic plane are responsible for the remarkable seasonal difference versus latitude in solar energy absorption in the atmosphere-earth system, with a significant even (odd) symmetric components around equinoxes (solstices); the surface inhomogeneity displays an appreciable odd symmetry, as shown by land-sea contrast in both hemispheres, with the land area ratio of the two hemispheres being 2:1 and its geographic distribution being of sole form (Tchernia 1980). It can be assumed that mean circulation OES is the result of joint effects of the above factors.

Previous studies concerning mean circulation OES reported their findings in aspects of symmetric and asymmetric motions in a barotropic filtering model (Liao et al. 1986), numerical simulation of such motions in a barotropic atmosphere (Yu et al. 1990), physical properties

* The study is supported by the Chinese Research Project of Long-Term Weather Prediction Theory and Techniques.

of these motions with their energy conversion (Liao et al. 1990; Wang et al. 1990) and analysis of stratospheric Kelvin and mixed Rossby-gravity waves at tropical latitudes (Yang 1991). All these aim at exploring the nature of mean circulation OES theoretically and using numerically simulating schemes. And their results help us gain insight into the mechanisms of circulation change. On the other hand, little has been reported about the investigation of tropospheric OES climatic features on a global basis by use of observations. Then, problems arise: What are these features? Is there any possibility that ENSO, for instance, as a local anomalous event of tropical sea temperature will give rise to pronounced anomaly in the OES components?

This paper focuses on the climatic features of mean circulation OES and the diagnosis of OES abnormality with main results will be presented in a separate article.

II. THEORETICAL BASIS

For φ in any scalar function $F(\lambda, \varphi, P, t)$, we have

$$F(\lambda, \varphi, P, t) = F_e(\lambda, \varphi, P, t) + F_o(\lambda, \varphi, P, t), \quad (1)$$

For $\varphi = 0$, F_e (F_o) denotes an even (odd) symmetric component that satisfy

$$F_e(\lambda, \varphi, P, t) = \frac{1}{2}[F(\lambda, \varphi, P, t) + F(\lambda, -\varphi, P, t)],$$

$$F_o(\lambda, \varphi, P, t) = \frac{1}{2}[F(\lambda, \varphi, P, t) - F(\lambda, -\varphi, P, t)] \quad (2)$$

with $\varphi = 0$ for the latitude of the equator. Thus, it is easy to put (1) and (2) into the atmospheric dynamic equations and then to examine their meanings (Liao et al. 1990; Wang et al. 1990). For these equations the readers can refer to their papers.

Following these considerations, a focus is on the interaction between the symmetric components and the results of time-varying changes and distributions of these components as basic elements for circulation characteristics.

III. CLIMATIC FEATURES OF OES PATTERNS BASED ON OBSERVATIONAL FACTS

Using the decompositions of the odd and even components and 1980—1986 monthly mean gridded data, analysis is performed of geopotential height Φ , temperature T , zonal (meridional) wind $U(V)$ and the global distribution of the odd and even components of the composite wind-vectors symmetric about the equator.

1. *Odd and Even Component Distribution Features ($\Phi = \Phi_o + \Phi_e$) Displayed by Geopotential Height*

Figure 1 portrays the Northern Hemisphere distributions of odd and even components in the Φ field in winter and summer.

Evidently, the even component plots show zonal-type patterns of the circulations except some difference in their strength between winter and summer and at not too low latitudes the Φ isoline pattern shows, the symmetric structure of basic flow (westerly wind) in both hemispheres. However, the odd-symmetric plot gives a rather complicated pattern of Φ horizontally, i.e., in northern winter, Φ is higher north of 60°N than south of 60°S , with an opposite case at midlatitudes, and at tropics Φ is bigger in the Northern than in the Southern Hemisphere, while, in northern summer, Φ is greater in the Northern Hemisphere than that at southern related latitudes, forming a situation with Φ and thus the odd component pattern, on the whole, higher

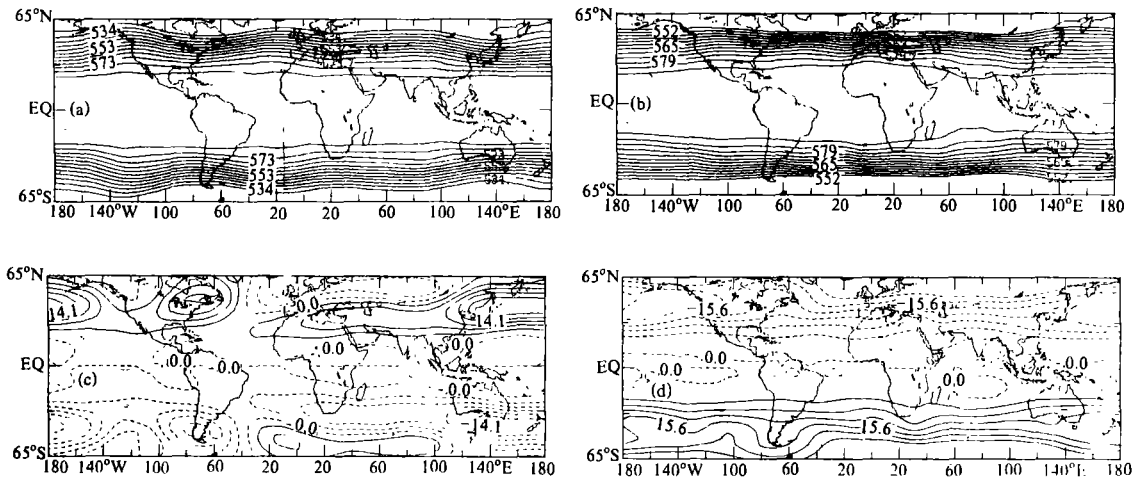


Fig. 1. 7-year (1980—1986) mean Φ odd (even) components for January and July shown in Figs. 1c and 1d (Figs. 1a and 1b). Note that solid (broken) line denotes a positive (negative) value in Figs. 1a and 1b as opposed to the case in Figs. 1c and 1d, which will be the same in the following figures.

in the Northern Hemisphere and the circulation in a straight form. Inspection of the 12-month evolution indicates that over midlatitudes of North America, Europe and the Pacific the weakening low-value area turns in May into a pattern typical of summer and of winter in November. The distinctive distribution and evolution of an odd type is obviously related to dynamic effects and difference in solar radiation absorption resulting from the land distribution discrepancy of both hemispheres while the zonal structures of the odd and even symmetric circulations are associated with the state of corresponding quasi-stationary waves on a monthly mean basis of the hemispheres.

We define the index of the symmetry for both hemisphere circulations as $I_{o\Phi} = \Phi_{\text{omax}} - \Phi_{\text{omin}} = 2|\Phi_{\text{omin}}|$, where Φ_{omax} and Φ_{omin} are the maximum and minimum of the odd symmetric component Φ_o , respectively, over the belt of 65°N—65°S. For this belt of Fig. 1, changes in I_o are listed in Table 1.

Table 1. Changes of Odd Symmetry ($I_{o\Phi}$) for both Hemispheres (units: potential decameter)

Month	Jan.	Feb.	Mar.	Apr.	May	Jun.	Jul.	Aug.	Sep.	Oct.	Nov.	Dec.
$I_{o\Phi}$	42.3	46.7	39.4	19.2	31.4	40.4	46.8	51.3	42.2	31.8	19.2	32.6

It is apparent that the strongest northern-southern asymmetry occurs in February and August in the seasonal transition for circulations, with the weakest odd symmetry in April and November. From Table 1 one can find the time scale of atmospheric reponse to external forcing governed by dynamic processes inside the atmosphere in relation to solar energy change and atmosphere-underlying surface interaction. If the property of underlying surface is exactly the same in both hemispheres, then the genesis of the odd symmetric component and its change in magnitude ought to be controlled by such major anomalous events as ENSO, and internal dynamic processes (nonlinear), leading to an one-month or so time scale of atmospheric response to radiation forcing. This is a generally accepted outcome and in agreement with the maximum

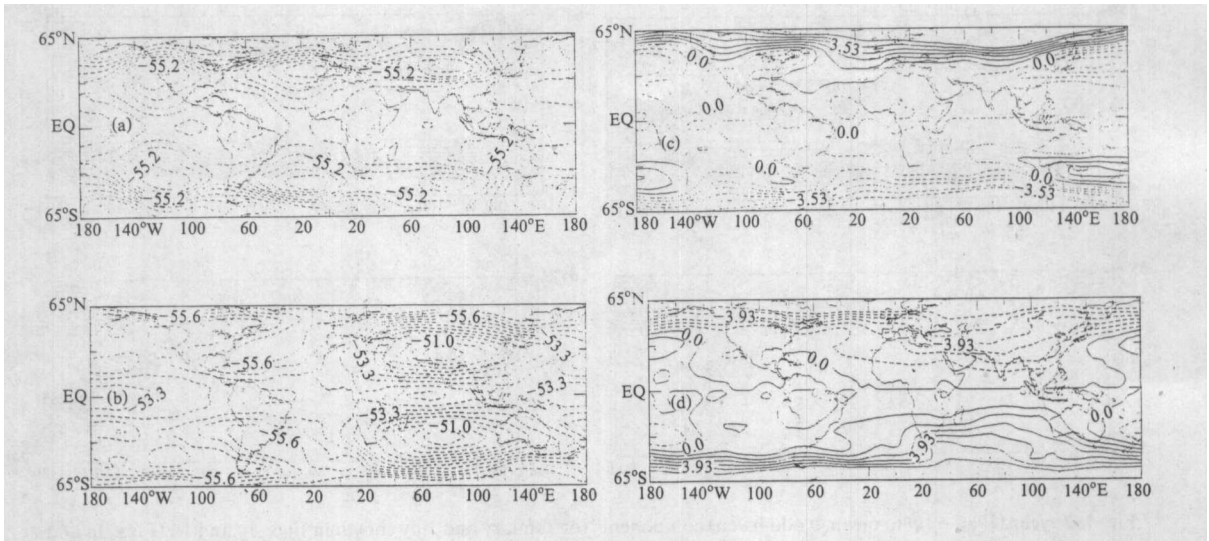


Fig. 2. 200-hPa temperature field odd and even symmetric component patterns for January and July, with the even (odd) component T_e (T_o) shown in Fig. 2a and 2b (2c and 2d).

of $I_{o\phi}$ around solstices but the first minimum happens soon after vernal equinox (March 21) and the second in November far behind autumnal equinox (September 23), which seems to show that the period of atmospheric response is longer in fall than in spring, possibly related to the different initial states at equinoxes.

It is evident from Table 1 that the time-dependent variation of $I_{o\phi}$ is marked by pronounced discrepancy in winter to summer transition, with $|I_{o\phi, i+1} - I_{o\phi, i}|$ reaching 20.2 between May and April and < 13.4 for other month-to-month spans, indicating that the most intense adjustment of global circulations takes place subsequent to vernal equinox. $I_{o\phi}$ is more vigorous in August than in February, which dicates clearly different contribution of winter monsoon activities to the odd symmetry of both hemisphere circulations.

The above results are found from 200 hPa height analysis as well. For space limitations of the paper they are not presented here.

2. Odd and Even Symmetric Components ($T = T_e + T_o$) Displayed by 200-hPa Temperature Plots

Figure 2 depicts the OES for January and July over the 200 hPa temperature fields.

It is evident from the figure that in northern midlatitude winter triwave disturbance is clearly revealed with the centers located, separately, over the eastern Pacific, eastern Atlantic and Qinghai-Xizang Plateau. As summer approaches the above cold centers orientated zonally get weakened and along 70°E a pair of vigorous warm centers is symmetry with a cold center over equatorial latitudes, a situation that is intimately associated with monsoon activities. The northern 70°E warm center forms as it intensifies and shifts northward from equatorial 100°E in May to June.

From Figs 2c and 2d one sees that the northern winter temperature north of 50°N and over the Pacific/Atlantic north of 20°N is lower than in the related belts in the Southern Hemisphere, so is that southward of 20°N as compared to SH tropical latitudes. On the other hand, it is warmer over the midlatitude North Pacific than over its southern counterparts. The

reversal happens in July so that seasonal shift makes for an anti-phase change over the Pacific. The turning from January to July takes place between May and April, starting from the polar regions to the north (south) of 60°N (60°S) and marked by the northward advance of the Pacific cold sector south of 20°N and by disintegration of the Eurasian cold area in May. The complete reversal from the winter to summer patterns occurs in June. On the other hand, in the turning from the July to January patterns the strongest cooling begins first over Eurasia at $30\text{--}50^{\circ}\text{N}$ with the full reversal observed in December. Inspection of the odd symmetric strength shows that it is most vigorous (feeble) in January and July (April and October), which differs from the height field regarding the change features.

Therefore, consideration of atmospheric temperature adjustment in seasonal transition of global circulation patterns should be focused on the changes in polar regions (from spring to summer) and in midlatitude Eurasia (from summer to winter). The related figures are not shown here.

3. Analysis of Zonal Flow Components ($u = U_e - U_o$)

Shown in the following 200 hPa diagram are the OES components of zonal flow by decomposing zonal wind actually observed.

It can be seen from Figs. 3a and 3b that the westerly jet core in January is situated at the longitudes of the western Pacific and coastal belts of China, with the west wind still blowing over the Atlantic and eastern Pacific while in July the west wind is weakened with the center moved westward to around 80°E , and under the influence of Asian monsoon an east wind region show up over the Indian Ocean with other parts around the equator under the control of easterly flow, too. Therein one can discern a salient feature that a major westerly jet core is

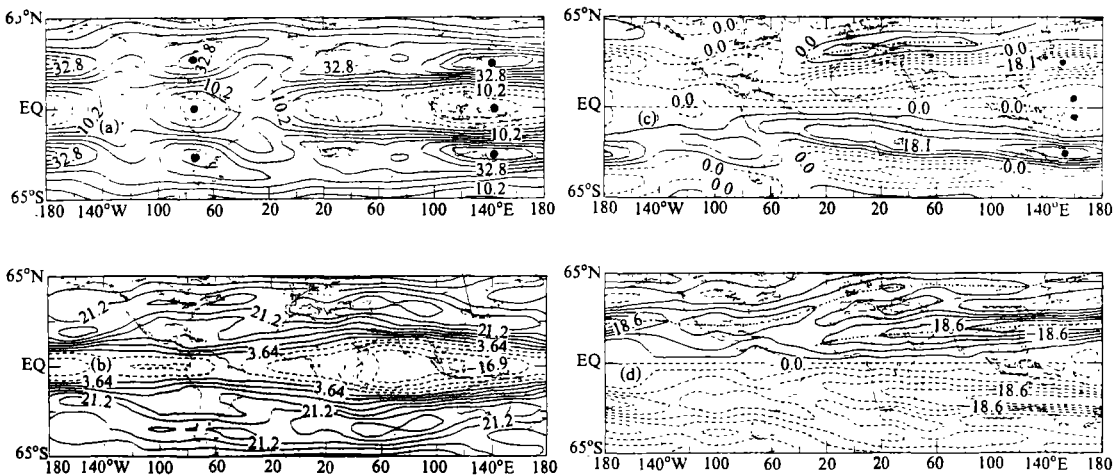


Fig. 3. Plots of zonal wind OES components averaged over 1980—1986 for January and July where Figs. 3a and 3b denote even component pattern with solid (broken) line representing a positive (negative) value as opposed to the case of Figs. 3c and 3d for odd component patterns.

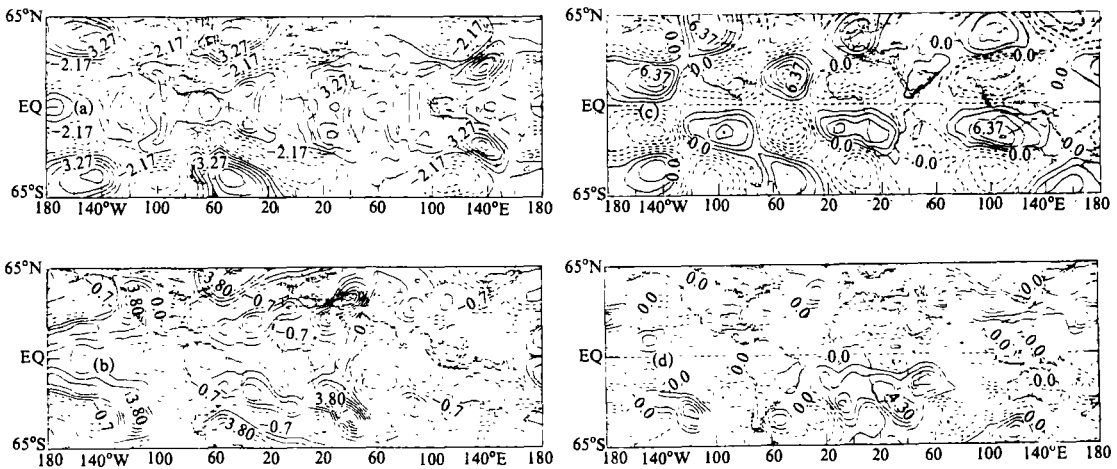


Fig. 4. 1980–1986 monthly mean charts of meridional wind OES patterns for January and July, with the same definition of contours as in Fig. 3.

collocated with a high-value east wind region at the same longitudes, meaning that the perturbation of zonal flow even symmetric components is characterized by noticeable meridional alignment.

However, the odd component patterns indicate the asymmetry of zonal flow in both hemispheres. For the northern winter (southern summer) the low and high latitude westerly flow is stronger in the northern than in the Southern Hemisphere, with a midlatitude easterly compensation belt in between, and the west wind observed in this belt is weaker in the Northern Hemisphere. All these are reversed when the Northern Hemisphere is in summer, where, except a meridionally arranged structure of perturbation as in the case of the even symmetric circulations, there is a conspicuous characteristic for the odd symmetric easterly flow showing a trend to follow a curved path towards the north in the Northern Hemisphere, a fact that is clearly revealed by each of the monthly mean charts (only those for January and July are presented in this paper), with the course starting from the Atlantic (denoted by the dotted line of Fig. 3d) and ending north of or around 65°N.

4. Analysis of Meridional Flow ($v = v_e + v_o$)

The OES of the vector field is defined (in relation to the streamfunction field) as $V_e = u_e i + V_o j$ and $V_o = u_o i + V_e j$ from the decomposition of the scalar v , with the results of 200 hPa meridional flow decomposition shown in Fig. 4.

It is obvious from the even symmetric component (southerly vector of the odd component) plots that the northern winter meridional motion displays a bi-wave feature at higher latitudes, i.e., a south (north) wind belt is found over the Pacific and Atlantic extratropics (over the continents); at equatorial latitudes there appear three strong south wind regions located, separately, over 100–120°W, 5–40°E and 60–150°E. In connection with monsoon the south flow over the Asian monsoon area is changed in July into a southward cross equatorial flow, so is the case with Mexican monsoon in corresponding area but the change is faint for Africa. The strongest

south wind in January is observed at low and mid latitudes of 140°E and midlatitudes of 50°W , and in July around (30°N , 40°E) and (30°S , 40°E). The even component diagrams illustrate that the zonal alignment of the perturbation structure is much clearer at extratropics than at low latitudes.

From the odd symmetric (the vector field of the even symmetric) component charts we can see that of interest is the meridional wind perturbation displayed by the January plot, where in the area delineated by 32.5°N and 32.5°S , two belts of a positive center alternated with a negative one, symmetric about the equator, are shown but in opposite phase. On the plots one sees a zonal (meridional) tri- (bi-) wave structure, a characteristic that differs from that of the even symmetric charts. At the equator where $V_0 = 0$, it can be assumed that convergence and divergence have a tri-wave structure as well.

As summer falls on the Northern Hemisphere, the odd symmetric meridional wind perturbation gets decreased, with an ill-defined zonal arrangement of the perturbation structure at low latitudes except that the zonal structure around $\pm 35^{\circ}$ remains quite clear.

IV. INTERPRETATIONS AND RELATIONS

So far we have given the description of the principal features of OES component patterns of the different elements revealed by the monthly mean charts averaged over 1980—1986. It needs further elucidation of the production of these features and the relations between the fields of these quantities. Though derived mathematically, the OES patterns reflect the OES waves coming from the decomposition of Fourier or spheric function. For the global circulation as a whole, some but no particular attention has been paid to the difference and similarity in circulation patterns between both hemispheres in previous studies. As shown in Matsuno (1966) and Yang (1991), equatorial Kelvin wave as the result from a dynamic model of even symmetric components and equatorial Rossby - gravity waves given by synchronous OES analysis present a useful description of low-latitude atmospheric wave and it is found that the response to the forcing of equatorial SST anomaly gives rise to the anomalous structures in both hemispheres as even symmetric patterns. It follows that the long-term monthly mean OES results from interaction between the two hemispheres, waves inside the atmosphere and physical quantity transport under the effects of solar forcing and discrepancy in land-sea discrepancy of both hemispheres. Further analysis is given below.

(1) The distribution of even symmetric components reveals a basic structure of circulations on a global basis, for example the basic westerlies at extratropics. And the difference in monthly means for January and July indicates the influence of land-sea discrepancy of both hemispheres.

(2) The distribution of odd components is indicative of atmospheric motion with its seasonal change, and the incomplete reversal of the patterns for January and July for both hemispheres shows the substantial effects of their land-sea discrepancy. Further, the difference in data between the equinox (spring and autumn) and the day when odd symmetry reaches its maximum displays the time scale of the atmospheric response to thermal forcing caused by solar radiation.

(3) The meridional alignment of jet cores (Figs. 3a and 3b) exhibits the consistency of flow intensity change in space controlled by horizontal quasi-incompression on the north / south sides of cyclonic or anticyclonic circulation centers, and the structure of odd symmetric

meridional wind (the vector pattern of even components) perturbation displays a two-dimensional wave feature in the atmosphere.

(4) In the interaction of two hemispheres, the meridional wind component of the even symmetry pattern (the meridional wind vector of the odd pattern) represents cross-equatorial flow, responsible for the exchange of mass, momentum and energy between the hemispheres. In view of the fact that the exchange attains a maximum over the equator, the even component meridional wind makes no contribution to the vertical circulations of those latitudes.

(5) The January—July global circulation adjustment begins from polar regions, which should be related to the reversal of their reception of solar energy. And the vicissitude in westerly flow in association with the geopotential height is harnessed by ageostrophic relation. The odd—even pattern interplay (Liao et al. 1990; Wang et al. 1990) indicates the mutual dependence of both components in their variation in the course of the changing circulations for both hemispheres.

V. CONCLUDING REMARKS

OES analysis for both hemispheres consists mathematically of separate treatments of the odd and even symmetric components from the expansion of spheric function, and physically of investigation of two orthogonal components of a meridional structure of a circulation. Through the decomposition of the atmospheric dynamic equations we get to know that the global circulations as a whole have their variations reflected in the two kinds of components. The exploration of climatic features given by OES based upon observations indicates that the odd and even component patterns with their vicissitude may serve to uncover the effects of both hemispheric land-sea discrepancy and monsoon activities, the time scale of atmospheric response to solar radiation forcing in different seasons, atmospheric large-scale wave structure, etc.

A further examination of the index for measuring the OES with its relation to major climatic anomalous events on a global basis will be dealt with in the sequel of this paper.

REFERENCES

- Liao Dongxian et al. (1986), On symmetry and anti-symmetry in a barotropical filtering model, *Acta Meteor. Sin.*, **44**: 28—36 (in Chinese).
- Liao Dongxian et al. (1990), On physical properties of symmetric and anti-symmetric motions and their energy conversion, *Acta Meteor. Sin.*, **48**: 385—395 (in Chinese).
- Matsuno, T. (1966), Quasi-geostrophic motions in the equatorial area, *J. Meteor. Soc. Japan*, **44**: 25—43.
- Palman, E. and Newton C. W. (1969), *Atmospheric Circulation System*, Academic Press.
- Pogoxin, H. P. (1972), *Atmospheric Circulation*, Hydrometeor. Press, Moscow (in Russian).
- Tchernia, P. (1980), *Descriptive Regional Oceanography*, Pergamon Press.
- Wang Shiwen et al. (1990), Analysis of rationality of a multi-level primitive equation model, *Collection of Papers on Medium-Term Numerical Prediction*, Chinese Academic Press, **4**: 71—87 (in Chinese).
- Yeh Tsuzheng and Zhu Baozhen (1958), *Some Basic Problems on Atmospheric Circulation*, Scientific Press, Beijing (in Chinese).
- Yang Yunfeng (1991), Symmetric and anti-symmetric motion in the lower stratosphere over tropics, *Sci. Atmos. Sin.*, **15**: 77—86 (in Chinese).
- Yu Hai'an et al. (1990), Numerical simulation of symmetric and asymmetric motions in barotropical atmosphere, *Acta Meteor. Sin.*, **48**: 284—292 (in Chinese).